Pergamon
www.elsevier.nl/locate/asr

*Adv. Space Res.* Vol. 23, No. 7, pp. 1217–1224, 1999

Printed in Great Britain
0273-1177/99 $20.00 + 0.00

PII: S0273-1177(99)00187-8

# EJECTION VELOCITIES OF ICE FRAGMENTS IN OBLIQUE IMPACTS OF ICE SPHERES

Masahiko Arakawa

*Institute of Low Temperature Science, Hokkaido University, Sapporo 060-0819, Japan*

## ABSTRACT

Reaccumulation conditions of icy planetesimals in collisional disruption were studied experimentally using a one-stage light gas gun set in a cold room (-18°C). Oblique impacts between ice spheres were used to measure the velocity distributions of fragments. The impact velocities ranged from 170 to 640 m/s, and the projectile-to-target mass ratio was a constant and equal to 0.13. The collisional disruption was observed by ultra-high speed photography at a rate of $2 \times 10^5$ to $1 \times 10^4$ frames/s. As a result, we found that the minimum ejection velocity was related to the specific energy and the impact angle by: $V_{min} = 0.092 Q'^{0.65}$, where $Q' \equiv Q(\cos\theta)^5$. $Q$ is the specific energy defined as a ratio of projectile kinetic energy to target mass. On the other hand, high velocity ejecta caused by jetting was observed around the impact point, and the normalized maximum velocity was found to range from 1.6 to 3.1, irrespective of impact angle and impact velocity. The reaccumulation conditions were estimated in oblique impacts of 480 m/s with a mass ratio of 0.13 by comparing the ejecta velocity with the escape velocity of the icy planet. As a result, it was clarified that icy planets with radii larger than 100 km can capture most of the fragments in collisions with impact angles from 0 to 50°.



## INTRODUCTION

Recent planetary exploration by spacecraft such as Voyager and Galileo has revealed that there are many icy planets with a variety of compositions in the outer solar system. As a result of these observations, water ice is believed to be one of the most abundant volatile materials in icy planets. Therefore, when we consider the growth process of icy planets in the proto-solar nebula, it is very important to study the collisional accretion process of icy planetesimals. When two icy planetesimals collide with each other, they are disrupted and many fragments that have been formed by the impact pressure are ejected. The fragments with a velocity lower than the escape velocity ($V_{esc}$) of the planetesimal can be captured by gravity; as a result, the captured fragments form a planet with an internal structure like a 'rubble-pile' consisting of reaccumulated fragments (Chapman *et al.*, 1989), and the escaped small fragments form an icy dust postulated to lie in the Kuiper belt region (Yamamoto and Mukai, 1998). A quantitative study of the velocity distribution of ice fragments is therefore necessary to investigate the planetary accretion process. High velocity impacts on ice targets have been studied by several groups (Kato *et al.*, 1992; 1995; Lange and Ahrens, 1987), and the velocity distribution of the disrupted fragments have also been studied by impact experiments and numerical simulations for silicate materials (Asphaug and Melosh, 1993; Fujiwara and Tsukamoto, 1980; Nakamura and Fujiwara, 1991).

Arakawa *et al.* (1995) have observed the antipodal velocity and the maximum fragment masses of targets in ice-to-ice collisions. Their systematic study determined the reaccumulation conditions for ice ejecta in head-on collisions, although, the observed antipodal velocity was limited to 20 m/s. Later, Arakawa and Higa (1996) measured ejecta velocity higher than the impact velocity by using ultra-high speed photography. They used ice spheres for both projectiles and targets in head-on collisions, and they observed the collisional disruption with a mass ratio of projectile-to-target near 0.1. In addition, the importance of oblique impacts in planetary accretion has been

suggested, and many studies of oblique impacts have been made in order to clarify this physical process. As a result, it has been shown that jetting frequently occurs during oblique impacts (Vickery, 1993). Vickery has theoretically studied the jetting of spherical projectiles impacting on a semi-infinite body and has successfully derived the ejecta distribution by jetting at various impact angles. The jetting of ice has also been theoretically studied by McKinnon (1989). He has calculated the critical angle above which the jetting occurs and has shown the dependence on impact velocity for impact melting and vaporization. However, there has been little experimental study of oblique impacts for ice.

At the initial stage of the accretion process of planets, the size ratio of the colliding bodies may be close to unity, and oblique impacts for these planets may thus occur frequently. We concentrate our study here on oblique impacts between ice balls of almost the same diameter. In order to determine the reaccumulation conditions for colliding ice bodies, we studied the following: (1) the velocity distribution of ejecta, which means the relation between the initial position of the fragments and the fragment velocities; (2) the dependence of the ejecta velocity on the impact conditions, especially the dependence on the impact angle and the impact velocity at a constant mass ratio of projectile-to-target. To carry out our study of these issues, laboratory experiments on the collisional disruption of ice were made in a cold room.

## EXPERIMENTAL METHOD

Spherical ice balls were prepared as both projectiles and targets for the collisional experiments. Both samples were made of a columnar polycrystalline ice in which the crystals are elongated in the direction of the crystallographic $a$-axis. The crystal size was about 1 cm. The samples were made from an ice block formed in a spherical mold. The diameter of the spherical projectiles was 15 mm (mass 1.5 g) and that of the targets was 30 mm (mass 12 g). The projectile-to-target mass ratio remained constant (0.13).

**Table 1. Experimental Conditions and Results**

| Run No. | $V_i$ (m/s) | $\theta$ (°) | $V_{jet}/V_i$ | $V_{min}$ (m/s) | $Q$ (J/kg) | $Q'$ (J/kg) | References |
|---|---|---|---|---|---|---|---|
| 941027-4 | 470 | 0 | n.d. | 48.3 | 12591 | 12591 | A&H |
| 950705-2 | 496 | 0 | 2.7 | 56.3 | 15056 | 15056 | |
| 960523-2 | 472 | 7 | 2.3 | 53.0 | 14767 | 14225 | |
| 950705-4 | 516 | 18 | 2.9 | 35.5 | 17232 | 13408 | |
| 960523-3 | 475 | 30 | 2.6 | 27.2 | 15630 | 7614 | |
| 960522-1 | 460 | 47 | 2.6 | 12.0 | 13161 | 1941 | |
| 950705-5 | 485 | 48 | 2.5 | 15.3 | 14993 | 2011 | |
| 960523-4 | 455 | 50 | 2.7 | 10.2 | 12956 | 1421 | |
| 960522-5 | 171 | 41 | 2.4 | 5.88 | 1989 | 487 | |
| 960521-1 | 248 | 45 | 2.6 | 5.25 | 4440 | 784 | |
| 960522-2 | 329 | 40 | 2.6 | 12.1 | 7378 | 1946 | |
| 960522-4 | 540 | 45 | 1.6 | 19.6 | 19098 | 3376 | |
| 960522-7 | 641 | 36 | 2.2 | 30.5 | 25813 | 8946 | |
| 941027-1 | 153 | 0 | 3.1 | n.d. | 1498 | 1498 | A&H |
| 950705-3 | 176 | 0 | 2.9 | 14.0 | 1903 | 1903 | |
| 941027-2 | 246 | 0 | 1.9 | 27.8 | 3843 | 3843 | A&H |
| 950704-5 | 246 | 0 | 2.6 | 18.4 | 3814 | 3814 | |
| 941027-3 | 333 | 0 | 2.7 | 25.5 | 7096 | 7096 | A&H |
| 950705-1 | 362 | 0 | 2.5 | 26.6 | 8846 | 8846 | |
| 941027-4 | 470 | 0 | n.d. | 48.3 | 12591 | 12591 | A&H |
| 941027-5 | 575 | 0 | 2.9 | 54.5 | 20333 | 20333 | A&H |
| 941028-1 | 687 | 0 | 1.9 | 73.5 | 31622 | 31622 | A&H |

$V_i$ and $\theta$ are the impact velocity and the impact angle respectively. $V_{jet}$ is the maximum jet velocity at the downstream. $V_{min}$ is the minimum ejection velocity of the target far from the impact point. $Q$ and $Q'$ are the specific energy and the modified specific energy respectively. A&H is Arakawa and Higa (1996).

The ice projectile was launched by a one-stage light gas gun with a launch velocity between 170 m/s and 640 m/s. The gun was installed in a large cold room regulated at −18°C. The target was hung by thin strings in an acrylic resin sample box. The sample box was placed in a chamber evacuated at $10^4$ Pa. The impact angle between the projectile and the target was from 0 (head-on collision) to 60° (Table 1).

Collisional disruption was observed by ultra-high speed photography using an image-converter camera (Arakawa and Higa, 1996). Twelve images were photographed and these images were recorded at a rate from $2x10^5$ to $1x10^4$ frames/s, which corresponds to a recording interval from 5 μs to 100 μs. An exposure time shorter than 1 μs is necessary to take a still image of a moving object with a velocity of more than 1 km/s, so that a bright Xenon flash lamp with a pulse energy higher than 50 J per one pulse was used for illuminating the sample. The flashlight was concentrated by a pair of concave mirrors to make a parallel beam with a diameter of 15 cm. The shadow photograph technique was used to enhance the fragments using this parallel beam, and the shadow of the envelope made by the fragments was then observed by this technique. Although each fragment can't be resolved in the recorded image, the tiny high-speed fragments originated by jet can be easily observed by this technique because it is very sensitive to variations in the reflective index caused by the incidence of ice particles. A laser beam and a photodiode detector were used as a triggering system for this photography, in which the intensity of the laser beam would change when the launched projectile would pass through the beam. This intensity change occurred so quickly, within 10 μs, that it could be used as a trigger. The observation was made perpendicular to the impact direction. This means that the shadow projected on the impact plane was observed. The collisions were assumed to be plane symmetric and the symmetry plane is defined as the plane including the impact point and the centers of the projectile and target.

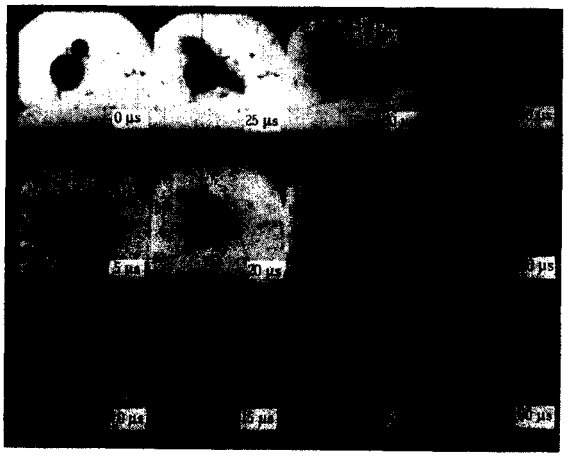


Fig.1. 12 successive images of the collisional disruption taken by the ultra-high speed photography. Impact velocity and angle are 641 m/s and 36° respectively.

## RESULTS

### Ultra-high Speed Photography

Figure 1 shows a photograph taken by the image-converter camera. The projectile collides with the target at a velocity of 641 m/s. The impact angle between them is 36°. The impact angle is defined as the angle between the impact direction and the normal direction. The normal direction is defined as a line linking the centers of the two spheres when the projectile and the target just contact each other (Fig. 2). After the contact, high-velocity fragments are ejected from the impact point perpendicular to the normal direction. The velocity of these ejecta exceeds the impact velocity by more than two times, and these ejecta may therefore be originated by jetting. The ejecta expand further to the lower side (the downstream direction) than the upper side (the upstream direction). The envelope made by the fragments far from the impact point expands after 80 μs. The envelope is almost symmetrical to the normal direction and not to the impact direction. We next choose this direction as one of the axes of a rectangular coordinate system in order to analyze the ejection velocity. The envelope of the shadow in the image at each time is traced to make a contour, as shown in Fig. 2. The expansion velocity of the envelope at each angle is measured along the line drawn from the impact point. The axis downstream perpendicular to the normal direction is defined as the base line, 0°. The angle is measured from this line in a clockwise direction. The velocity distribution of the

fragments ejected from the target surface must be measured at each position. However, the fragments are so small that the individual fragments can't be resolved on the image. We assume here that the fragments eject along the line of each angle and expand from the initial angle position. Under this assumption, the measured expansion velocity of the envelope corresponds to the ejection velocity of each fragment originating from the sample surface. This assumption is the same as that used for the "radial point model" proposed by Paolicchi *et al.* (1989). Nakamura and Fujiwara (1991) have observed oblique impacts of basalt and have shown that the fragments are ejected symmetrical to the normal direction. They have also found that the direction of the ejected fragments is almost radial from the impact point, as has been proposed by Paolicchi *et al.* (1989). The linear relation between the position of the envelope along the assumed ejected direction and time shows the accuracy of this assumption. Based on our observations, fragments ejected from the target interior such as core fragments can't be measured. The fragments from the interior usually have a lower velocity than the surface fragments. Therefore, the expansion velocity of the envelope measured here seems to correspond to the maximum velocity of the fragments ejected from each angle.

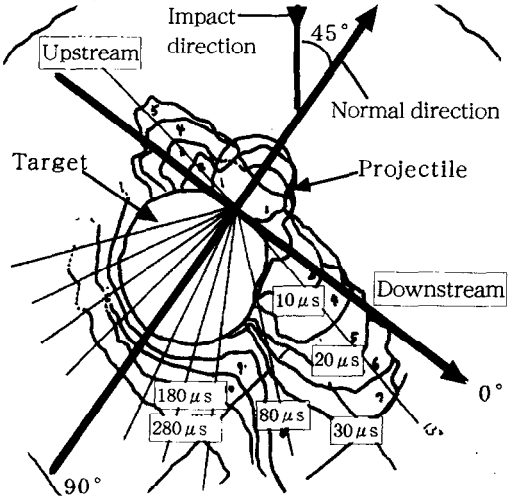


Fig.2. Counters of ejecta envelopes traced from the images in Fig. 1.

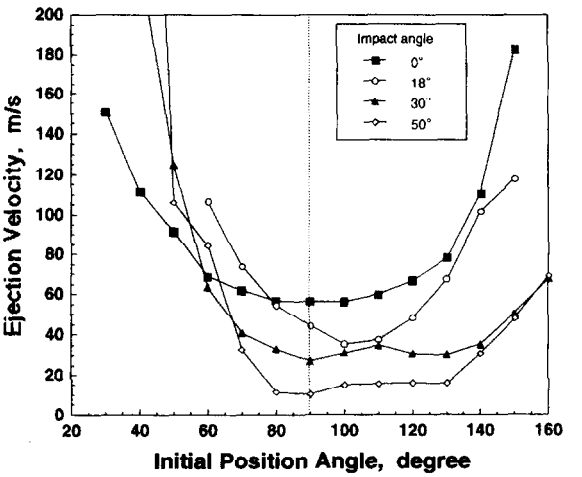


Fig.3. Velocity distribution of the collisional ejecta for the oblique impact. Impact velocity is constant, 480 m/

## Ejecta Far from the Impact Point

Figure 3 shows the velocity distribution of the fragments at each initial angle position. The results for different impact angles from 0 to 50° with the same impact velocity of 480 m/s are shown in this figure. The distribution is almost symmetrical to the initial angle position of 90° in the case of a head-on collision, and the minimum ejection velocity appears at the initial position of 90°; this position is on the opposite side of the impact point, and we call this initial position an 'antipodal point'. For the head-on collision, the antipodal velocity was found to closely correlate with the energy density ($Q$), defined as the kinetic energy of the projectile divided by the target mass (Arakawa and Higa, 1996 and Arakawa *et al.*, 1995). The relation between $V_{min}$ and $Q$ is determined for the data of Arakawa and Higa (1996) and our new results. It is described as

$$V_{min} = 0.16\, Q^{0.59}. \quad (1)$$

This relation is almost the same as that determined by Arakawa and Higa (1996) (Fig.4). The velocity distribution for oblique impact is different from that of the head-on collision. First of all, the minimum velocity decreases with increasing impact angle. The minimum velocity for a 50° impact is five times lower than that of the head-on collision. The position of the minimum velocity is not consistent with the antipodal point, and the velocity distribution is not symmetrical to the normal direction. The velocity in the downstream region is higher than that in the upstream region. The velocity with a large impact angle is larger than that with a lower impact angle at an initial angle position lower than 60°. On the other hand, the velocity with a large impact angle is almost constant between initial angle positions of 80° and 130°, and the velocity difference for the head-on collision becomes larger at an initial angle position larger than 130°.

The relation between the minimum velocity and the specific energy at a constant impact angle is shown in Fig. 4. The minimum ejection velocity for a 45° impact angle has a power-law relation to the specific energy, and the power-law index is slightly larger than that of the head-on collision. It is described as:

$$V_{min} = 0.03\, Q^{0.70}. \quad (2)$$

The velocity of the 45° impact angle is a half the velocity of the head-on collision in this energy density region. The impact-angle dependence of the minimum ejection velocity is shown in Fig.5 for a constant velocity of 480 m/s. The velocity along the normal direction, $V_i \cos\theta$, is important for the ejection velocity of the target because this component of the velocity compresses the target and induces a shock pressure which breaks and then accelerates the target fragments. We use this $\cos\theta$ as the scaling parameter. The minimum ejection velocity has a power-law relation to $\cos\theta$. The relation is described as:

$$V_{min}=49\,(\cos\theta)^{3.4}. \quad (3)$$

It is therefore clear that the minimum velocity for the variable impact velocities and angles are independently proportional to $Q^{0.7}$ and $\cos^{3.4}\theta$. According to this result, we assume a modified energy density $Q'$: $Q' \equiv Q(\cos\theta)^5$ as the scaling parameter for the minimum velocity. All obtained data are plotted with this parameter in Fig. 6. This figure shows the relation between the minimum ejection velocity and the modified energy density for our oblique and normal collisions. The relation is successfully described by the following empirical equation:

$$V_{min} = 0.092\, Q'^{0.65}. \quad (4)$$

Although $Q'$ is a rather empirical scaling parameter to arrange the data, this parameter may be key in describing the phenomena occurring far from the impact point.

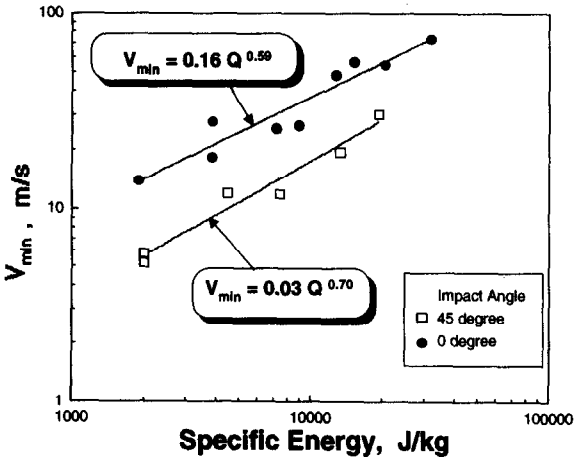


Fig.4. Minimum ejection velocity vs. specific energy for the collisions with a constant impact angle, 0 (head-on collision) and 45°.

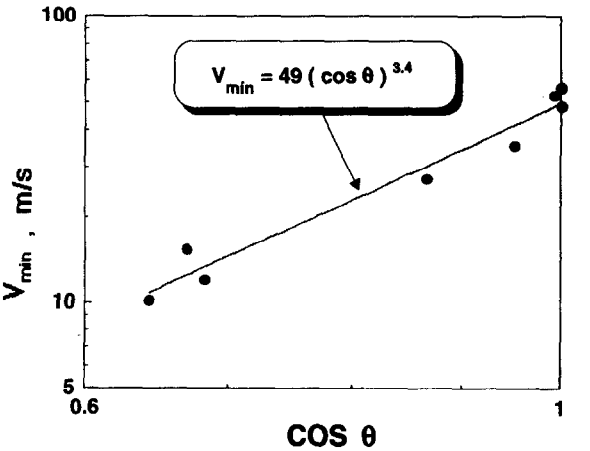


Fig.5. Minimum ejection velocity vs. impact angle for the collision with a constant impact velocity, 480 m/s. Impact angle varies from 0 to 50°.

## Ejection near Impact Point

The fine fragments ejected from the impact point are observed in Fig. 1, and the envelope that they form looks like a wing. The maximum velocity of this expanding envelope is measured from the impact point. In the case of oblique impacts, the velocity is higher downstream. We plot the maximum velocity in the downstream direction in Fig. 7. Figure 7 shows the measured velocity vs. impact velocity at various impact angles. The velocity is normalized by each impact velocity ($V_i$). In our velocity range, the normalized velocity ranges from 1.6 to 3.1. It is well known that high-velocity ejecta beyond the impact velocity appear in the oblique collision by jetting. We therefore call these high-velocity ejecta "jet".

The jet velocity of the head-on collision is almost constant, 2.5, irrespective of the impact velocity: the jet velocity is proportional to the impact velocity. The jet velocity of the oblique impact is also constant, 2.5, irrespective of the impact angle from 0 to 50° at an impact velocity of 480 m/s. However, a decrease in the jet velocity can be recognized at impact velocities higher than 600 m/s. The jetting process for impacts of spherical bodies oblique to the plane have been theoretically studied by Vickery (1993). Her study shows that the jet velocity varies according to the impact angle, with a maximum at about 30°. Our study does not show the clear dependence of the jetting velocity on the impact angle as shown in the study of Vickery, but decreases in the jetting velocity were found at large impact angles.

The anisotropy of jet speed dependent on the ejecta direction was also found in oblique impacts. The jetted material comes from both the projectile and the target and the ratio contributing to the jet is estimated by Vickery as being from 0.2 to 0.6. When we observe the ejecta originating from the projectile, the jetted material has a component of the initial velocity, which may explain the differences in the jet velocity in all directions.

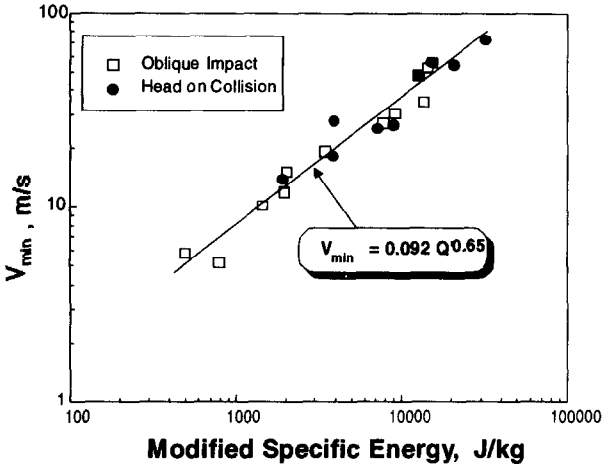


Fig.6. Minimum ejection velocity scaled by modified specific energy. The modified specific energy is expressed by $Q' \equiv Q(\cos\theta)^5$

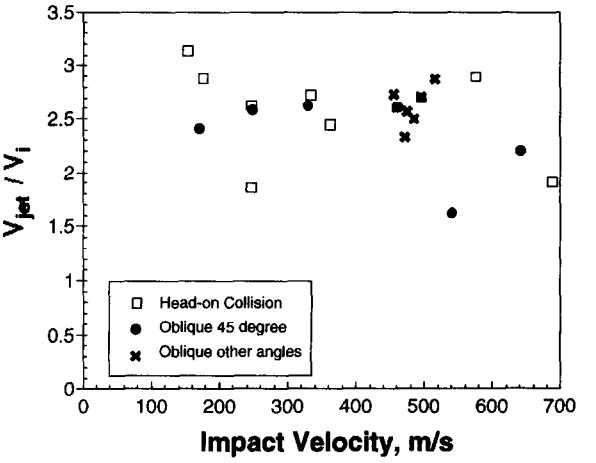


Fig.7. Normalized jetting velocity for the head-on collision and the oblique impact. The data of the oblique impact are divided into 45° impacts and the others.

## DISCUSSION

We clarified the ejecta velocity distribution of the spherules of oblique impacts, especially the jet velocity and the antipodal velocity when properly scaled by empirical parameters: $Q'$ and $V_i$. These parameters are very helpful in understanding the physics of the oblique impact; however when we apply our results to collisions among planets, the velocities of fragments should be changed from a laboratory system to a center-of-mass system. We can estimate the reaccumulation conditions by using the ejection velocity in the center-of-mass system: the fragments with a velocity lower than the escape velocity of the planet in the center-of-mass system can reaccumulate on the planet.

Figure 8 shows the velocity distribution in the center-of-mass system after an impact of 475 m/s with an impact angle of 30° (Run 960523-3). The direction of the velocity vector changes to the opposite side near the antipodal point, and the velocity is almost 0 m/s. After an oblique impact, the target is dragged by the projectile, and shear deformation occurs near the impact point. As a result, the target is extended in the impact direction.

Figure 9 shows the velocity distribution of the fragments at an impact angle of 0 to 50° in the center-of-mass system for an impact velocity of 480 m/s. It can be seen here that the velocity distribution for oblique impacts is different from that shown for a head-on collision in Fig. 3. In the case of a head-on collision, the velocity distribution is still symmetric to the normal direction, but the antipodal velocity becomes almost 0 m/s: the velocity of the center-of-mass is almost the same as the antipodal velocity, which has already been determined by Arakawa and Higa (1996). The velocity, except for the antipodal velocity, also becomes lower according to the initial angle positions. The velocity distribution of the oblique impact drastically changes in the center-of-mass system. The

initial position of the minimum ejection velocity, 0 m/s, varies from 90° for the head-on-collision to 60° for an oblique impact of 30°. However, in the case of impact angles larger than 30°, the minimum velocity becomes larger as the impact angle increases, reaching the same velocity as the center-of-mass, and the initial angle position for the minimum ejection velocity approaches the normal direction, 90°. With the maximum impact angle in this experiment, 50°, the minimum ejection velocity was approximated about 40 m/s, which is close to the velocity of the center-of-mass, 50 m/s.

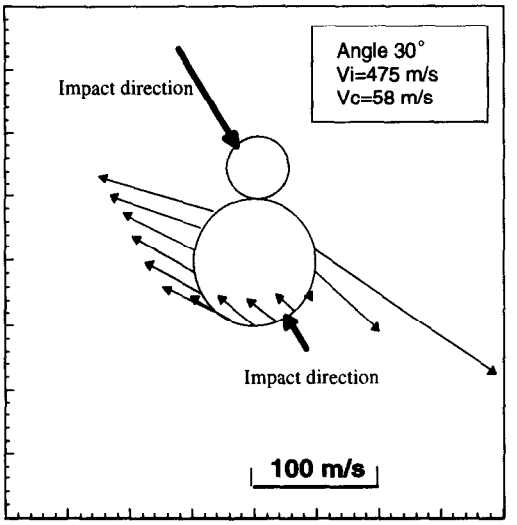


Fig.8. Velocity vectors of the collisional ejecta for Run 960523-3 in the center-of-mass system. Velocity of the center-of-mass ($V_c$) is 58 m/s.

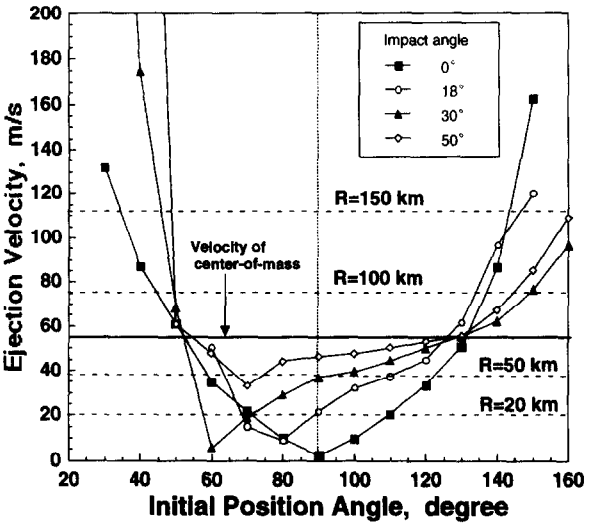


Fig.9. Reaccumulation conditions of ejecta far from the impact point in the oblique impact with 0 to 50° impact angle. Velocity of the center-of-mass is 55 m/s. $R$ is the radius of the icy planets with the density of 1000 kg/m$^3$. The ejecta with the velocity lower than the dashed line can accumulate on the planets by the self-gravity.

The ejecta velocity rapidly increases with distance from the initial position of the minimum ejection velocity. The ejection velocity at the upstream side rapidly increases from 0 to above 100 m/s. The slope of the distribution increases with increases in the impact angle. On the other hand, the ejection velocity on the downstream side gradually increases from 90 to 130°. The reaccumulation conditions were studied using Fig. 9 by assuming oblique collisions between icy planets with a density of 1000 kg/m$^3$, an impact velocity of 480 m/s, and a mass ratio of 0.13. The escape velocities of these planets are shown on this figure. For example, the planet with radius of 100 km has an escape velocity of 75 m/s. The escape velocity of each planet was compared with the velocity distribution

estimated from this study. As a result, in these collisions, a planet with a size of smaller than 20 km and has difficulty in capturing the fragments at all initial angle positions, especially at an impact angle of 50°, and planets smaller than 50 km can't capture the fragments at all. On the other hand, planets larger than 100 km can capture the fragments at a wide initial position between 30 and 130°. In these oblique collisions, when the escape velocity of the planets is higher than the velocity of the center-of-mass, the reaccumulation easily occurs.

## SUMMARY

We designed a laboratory experiment to examine the collision disruption of ice by using a one-stage light gas gun installed in a cold room. We especially studied the oblique collisions between ice balls with a large projectile-to-target mass ratio, 0.13 and measured the velocity distribution of ejecta by using ultra-high speed photography.

1. The minimum ejection velocity was dependent on the specific energy and the impact angle, and a scaling parameter including the impact angle was proposed.
2. The normalized maximum jet velocity ranged from 1.6 to 3.1 times the initial velocity, and it was almost independent on the impact angle.
3. Reaccumulation conditions were studied in oblique impacts at 480 m/s. The ejection velocity in the center-of-mass system was used, and it was clarified that an icy planet with an escape velocity higher than the center-of-mass could capture a lot of fragments from a wide range of initial angle positions.

## ACKNOWLEDGEMENTS

I greatly thank Prof. N. Maeno of the Institute of Low Temperature Science, Hokkaido University, for his useful comments regarding the experiment, and Dr M. Higa and Prof. M. Kato of the Institute of Space and Astronomical Science and S. Ichinohe of the Institute of Low Temperature Science, Hokkaido University, for their help in constructing the experimental apparatus and performing the experiment. I also thank S. Nakatsubo and T. Segawa of the Contribution Division of Institute of Low Temperature Science, Hokkaido University, for their technical help in carrying out the experiment.

## REFERENCES

Arakawa, M., and N. Maeno, M. Higa, Y. Iijima, and M. Kato, Ejection Velocity of Ice Impact Fragments, *ICARUS*, **118**, 341 (1995).

Arakawa, M., and M. Higa, Measurements of ejection velocities in collisional disruption of ice spheres, *Planet. Space Sci.*, **44**, 901 (1996).

Asphaug, E., and H. J. Melosh , The stickney impact of Phobos: a dynamical model, *ICARUS*, **101**, 144 (1993).

Chapman, C. R., P. Paolicchi, V. Zappala, R. P. Binzel, and J. F. Bell, Asteroid families: Physical properties and evolution, In *Asteroid II*, R. P. Binzel, T. Gehrels and M. S. Matthews ed., pp. 386-415, The University of Arizona Press, Tucson (1989).

Fujiwara, A., and A. Tsukamoto, Experimental study on the velocity of fragments in collisional breakup, *ICARUS*, **44**, 142 (1980).

Kato, M., Y. Iijima, M. Arakawa, Y. Okimura, A. Fujimura, N. Maeno, and H. Mizutani, Impact Experiment on Low Temperature Ice, In Physics and Chemistry of Ice, N. Maeno and T. Hondo Ed., pp. 237-244, Hokkaido Univ. Press (1992).

Kato, M., Y. Iijima, M. Arakawa, Y. Okimura, A. Fujimura, N. Maeno, and H. Mizutani, Ice-on-ice impact experiments, *ICARUS*, **133**, 423 (1995).

Lange, M., and T. J. Ahrens, Impact Experiments in Low-Temperature Ice, *ICARUS*, **69**,506 (1987).

McKinnon, W., Impact jetting of water ice, with application to the accretion of icy planetesimals and Pluto, *Geophys. Res. Lett.*, **16**, 1237 (1989).

Nakamura, A., and A. Fujiwara, Velocity distribution of fragments formed in a simulated collisional disruption, *ICARUS*, **92**, 132 (1991).

Paolicchi, P., A. Cellino, P. Farinella, and V. Zappala, A semiempirical model of catastrophic breakup processes, *ICARUS*, **77**, 187 (1989).

Vickery, A. M., The Theory of Jetting: Application to the Origin of Tektites, *ICARUS*, **105**, 441 (1993).

Yamamoto, S., and T. Mukai, Dust production by impacts of interstellar dust on Edgeworth-Kuiper Belt objects, *Astron. Astrophys.*, **329**, 785 (1998).